

# Characterization of Yield Stress Development of Cement Paste by Electrical Resistivity

Mbujje Joel Webster<sup>1</sup>, WEI Xiaosheng<sup>1\*</sup>, ZHOU Kongjin<sup>2</sup>

(1. School of Civil Engineering and Mechanics, Huazhong University of Science and Technology, Wuhan 430074, China; 2. State Key Laboratory of Silicate, Wuhan University of Technology, Wuhan 430070, China)

**Abstract:** Yield stress development of cement paste is potentially governed by percolation of 3-dimensional links formed by hydration products on the surface of the particles. It rises steadily at a gradual rate before a sudden increase in rate of growth. In this study, a method was proposed to predict the yield stress development based on the diameter of spread ( $D$ ) of mini slump cone test and gradient from electrical resistivity measurement ( $K_m$ ). To evaluate the significance of ( $D$ ) and ( $K_m$ ) in terms of yield stress, they were quantitatively compared to the initial yield stress ( $\tau_0$ ) and rate of yield stress growth ( $K$ ) obtained from a rheometer. A mathematical relationship between the yield stress of cement paste, diameter of spread and electrical resistivity characteristic gradient was developed. The equation developed can be used as an alternative method to estimate yield stress of cement paste.

**Key words:** fly ash; electrical resistivity; rheology; yield stress

## 1 Introduction

The increased interest in environmental conservation has generated considerable research on using fly ash, a solid waste of coal utilization, as a substitution for cement. To this end, improvement in durability, long term strength, reduction in cost among others has been put forward by several studies as key advantages of fly ash. However, its influence on rheology has mixed findings, for instance, Grzeszczyk *et al*<sup>[1]</sup> reported improved fluidity whereas Bouzoubaa<sup>[2]</sup> found the opposite effect. The mixed results can be explained by Uchikawa, Uchida and Ogawa<sup>[3]</sup> who found that the fluidity of fly ash is influenced by the specific weight, shape factors, and specific area which vary with the type and source of fly ash and porosity.

Furthermore, processes that involve supporting and shaping of concrete and mortar on sites are controlled by the development of yield stress which itself is not easily measurable but may be inferred simply from the setting times as determined by penetration methods, yield stress of cement paste or

by more sophisticated methods such as acoustic echo<sup>[4]</sup>, scanning electron microscopy<sup>[1]</sup> and conductivity measurements<sup>[5]</sup>. With the evolution of time, the hydration process proceeds and the inter-particle bonds increase, which renders the use of flow curves ineffective as shearing at high rates breaks the bonds and reports a lower value of yield stress thus it is more reasonable to employ oscillating rheometer measurements<sup>[6-9]</sup> and shearing at low strain rate<sup>[10-12]</sup> to follow the shear stress development without disturbing the structure of the paste. Within a few minutes of mixing, the mini slump cone<sup>[13,14]</sup>, a simple tool is extensively employed as a quick inexpensive measure of fluidity of cement pastes.

Several models exist showing the development of strength as a function of porosity. Backe *et al*<sup>[15]</sup> while discussing oil well cement proposed extrapolating the strength development at a later age (1-7 days) to a much earlier age (hours) after mixing and showed that although the models may not fit numerically, they exhibit a trend that is predictable. Considering the works by Powers<sup>[16]</sup> and Balshin<sup>[17]</sup>, this approach shows a positive relationship between the strength development, porosity decrease and degree of hydration which are all affected by time. Experimental work by Amziane *et al*<sup>[12]</sup> shows that yield stress develops gradually before increasing rapidly beyond a threshold value, and this process is visualized as a two stage process but can be fitted with an exponential curve. By

©Wuhan University of Technology and Springer Verlag Berlin Heidelberg 2017

(Received: July 20, 2016; Accepted: Sep. 4, 2016)

Mbujje Joel Webster: Ph D Candidate; E-mail: 1718644479@qq.com

\*Corresponding author: WEI Xiaosheng(魏小胜): Ph D; Prof.; E-mail: victorwei@hust.edu.cn

Funded by the National Natural Science Foundation of China (Nos. 51478200 and 51778257)

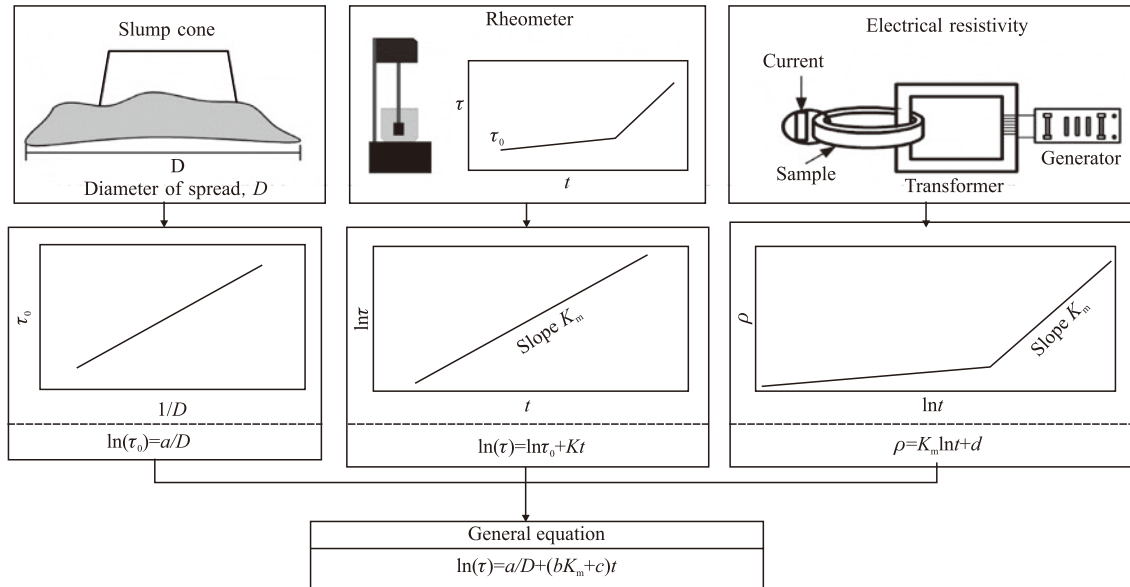


Fig.1 Determination of the relationship between diameter of spread  $D$ , yield stress and resistivity response

Table 1 Oxide compositions for cement and fly ash

Oxide	SiO <sub>2</sub>	Al <sub>2</sub> O <sub>3</sub>	Fe <sub>2</sub> O <sub>3</sub>	CaO	SO <sub>3</sub>	Na <sub>2</sub> O	K <sub>2</sub> O	MgO	LOI
Cement	5.17	3.22	0.94	65.08	24.69	/	/	/	0.9
Fly Ash	51.52	26.87	5.92	6.48	1.48	0.53	0.67	0.72	3.43

combining the assertions of literatures<sup>[12,15]</sup>, this study shows that the early development of yield stress can be modeled as an exponential function of time with rate of gain of stress ( $K$ ), and can be predicted from densification per unit volume ( $K_m$ ) which is determined from electrical resistivity.

The main objective of this study is to present electrical resistivity measurement as a sensing property for yield stress development and provide an alternative means of characterizing rheological development. Based on this method it is possible to narrow the choice of appropriate dosage of fly ash based on workability requirement by trial on paste used for concrete design. Electrical resistivity in this study is determined using a non contacting electrical resistivity method (NCERM) that has been the subject of study of many properties of cementitious materials<sup>[18,19]</sup> which eliminates contact problems faced when direct current apparatus is used and contact problems between the sample and probes. The specific methodology of this study is illustrated in Fig.1 and lists in steps (1), (2), and (3) as follows: Determine the yield stress development  $\tau(t)$  from rheometer, resistivity development  $\rho(t)$  from NCERM and diameter of spread  $D$  from mini cone; Calculate relationship between  $D$  and  $\tau_0$  from  $(\log\tau)-t$  and  $R$  from  $\rho-(\ln t)$ ; Yield stress can be estimated from Fig.1, where coefficients are experimentally determined.

## 2 Experimental

### 2.1 Sample preparation and mixing

Ordinary Portland cement, PO 52.5 and class III fly ash sourced from China were used. Their chemical compositions are given in Table 1. To ensure consistency in all the tests carried out, the temperature was controlled at 20±1 °C and the relative humidity at 95%±5%. Mixing was uniformly done for all the samples used in the tests using a laboratory planetary mixer, and slow mixing was carried out at 45 r/min for two minutes and at 90 r/min for a further two minutes with a break of 15 seconds to allow for scraping and cleaning. Tap water was used for all the tests. Samples were prepared with a water to binder ratio ( $w/b$ ) of 0.4 and fly ash replacement of 0%, 10%, and 20%. They are named as FA0, FA10, and FA20, respectively.

### 2.2 Rheometer measurements

The rheological behavior of each sample was measured using a Brookfield SST2000 rheometer with a four blade vane, 30 mm in height and 15 mm in diameter. The sample volume of 250 mL was sufficient to simulate an infinite medium<sup>[20]</sup>. To limit the evaporation of water from the paste, samples were placed in a chamber covered with a wet cloth between testing which was performed every 30 minutes. Before each measurement, the paste was remixed by hand to avoid settlement of particles and to provide a

homogenous paste, then left to rest for 30 seconds to dissipate residual stresses introduced by mixing, and afterwards the 0.01 r/min rotational rate was applied for 300 seconds. The yield stress  $\tau$  was the highest shear stress observed at a low shear rate of 0.01 r/min which produced reproducible results<sup>[21]</sup>.

### 2.3 Electrical resistivity

The apparatus adopted consisted of a generator, primary coil, polymer mould (secondary coil), current meter and computer as the main parts. Cement paste was cast into a polymer mold and the generator was switched on. The current by the generator passed through the primary coil and was induced across the sample; the current across the sample was calibrated according to Ohms law to give a measure of the resistance and thus the resistivity of the cement paste. More details about the principle of this apparatus can be found in the Ref.[22] and its operation is shown in the Ref.[18].

### 2.4 Fluidity

A truncated mini slump cone whose internal diameter was 36 mm at the top, 60 mm at the bottom with a height of 60 mm was used. Placed on a smooth ceramic tile, cement paste was poured until the brim of the cone; it was carefully carried up 6 minutes after gauging cement powder with paste. The paste was allowed to spread for a further 4 minutes before the diameter of the paste was measured along 2 perpendicular directions. The average of the two diameters was reported as the diameter of spread  $D$ .

### 2.5 Setting time and compressive strength

The setting time of the samples was determined as a supplementary test using a Vicat needle according to ASTM C191-08. The needle size was 1.13 mm with a load of 300 g, the joint between the test cone and the glass was made water tight using glycerin to prevent paste from leaking out. The compressive strengths of samples were determined at 1 day and 3 days. The specimens were cast in molds with dimensions of 40 mm×40 mm×40 mm and cured in a controlled chamber at 20±1 °C and relative humidity of 95%±5%. The specimens were tested using a hydraulic compressive machine at a loading rate of 2.4 kN/s.

## 3 Results and discussion

### 3.1 Rheometer measurements

Fig.2 shows the curve of shear stress against shear strain measured for sample FA10 at 210 minutes at a

constant shear rate of 0.01 r/min as described in the procedure. From Fig.2, it can be seen that the cement paste like other flocculated systems has an almost linear response of stress to an applied strain, until a maximum value beyond which the system does not completely recover and that is reported as the yield stress. From this curve, the yield stress  $\tau$  is 1212 Pa which is determined as the highest stress observed at a low shear rate of 0.01 r/min.

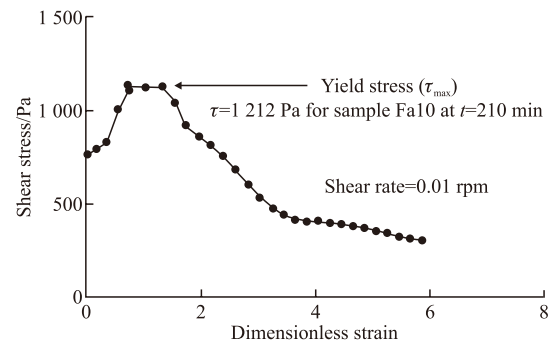


Fig.2 Yield stress measured for sample FA10 at 210 minutes at a constant shear rate of 0.01 r/min

The procedure is repeated for all the samples at intervals of 30 minutes. These yield stresses are plotted as a function of time. This procedure is used to determine the yield stress without disrupting the microstructure.

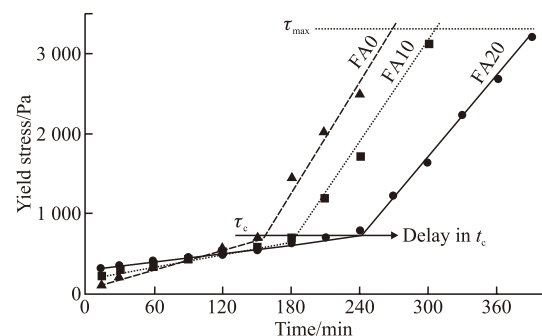


Fig.3 Time evolution of yield stress for all the samples

Fig.3 illustrates the yield stress  $\tau$  for all the samples as a function of the hydration time. The time evolution of yield stress for all the samples shows a gradual increase of yield stress up to a critical point  $\tau_c$  when there is a drastic change in slope. It should be noted that  $\tau_c$  is approximated from graphing since measurements on the samples are made every 30 minutes.

Fig.3 shows that the yield stress growth is a two stage process that has an intersection point at  $\tau_c$ . The value of  $\tau_c$  for all the 3 samples is approximately 850-900 Pa. The increased replacement of cement with fly ash causes a delay in critical time  $\tau_c$ . Initially at 15

minutes from gauging, FA20 has a higher initial yield stress  $\tau_0$  of 317 Pa. After the crossing point, FA0 has the highest yield stress compared with FA10 and FA20.

Fig.4 shows the transformation of yield stress corresponding to samples FA0, FA10, and FA20 respectively to the log scale. On the right axis are the actual values of yield stress  $\tau$  in Pascals.

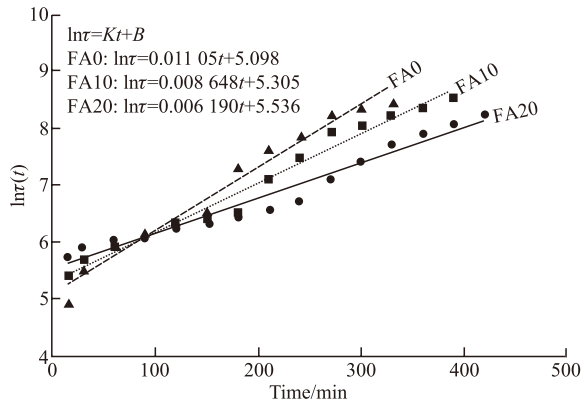


Fig.4 Yield stress development from rheometer (log scale)

The quantitative importance of slope  $K$  is calculated from Eqs.(1-4) and listed in Table 2.

Generally:  $\ln\tau = Kt + \ln\tau_0$  (1)

For FA0:  $\ln\tau = 0.01105t + 5.098$  (2)

For FA10:  $\ln\tau = 0.008648t + 5.305$  (3)

For FA20:  $\ln\tau = 0.006190t + 5.536$  (4)

The dependence of slope  $K$  on the amount of fly ash in the system is very evident. The lower slope with increased amount of fly ash can be accounted for by the reduction of cement hydration product because of partial cement replacement resulting in smaller number of contacts, retardation of hydration in the second stage of hydration and formation of weak bonds between cement and fly ash particles by the hydration products.

### 3.2 Electrical resistivity

Fig.5 shows the bulk resistivity of cement paste with fly ash replacements of 0%, 10%, and 20% after 24 hours of curing and it is observable that all the

samples follow a characteristic Sigmoid shape over 24 hours-the resistivity decreases slightly to a minimum  $\rho_m$  and maintains an almost level state for a few hours before a rapid increase in the setting area.

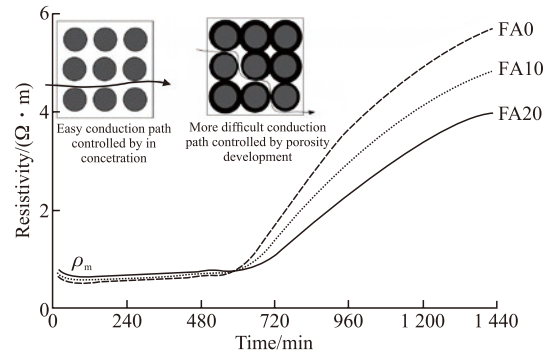


Fig.5 Electrical resistivity development for samples FA0, FA10, and FA20

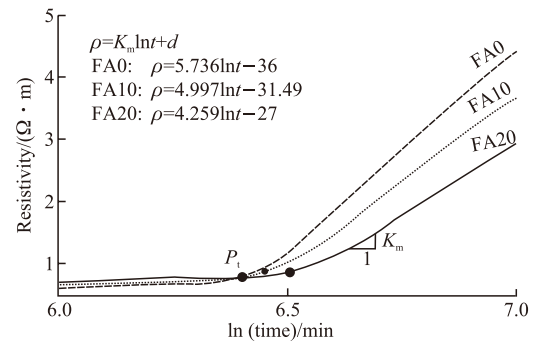


Fig.6 Electrical resistivity response showing transition point  $P_t$  and slope  $K_m$  (log scale)

The average minimum resistivity  $\rho_m$  of samples FA0, FA10, and FA20 are 0.521, 0.581, and 0.631  $\Omega\cdot m$  respectively as summarized in Table 2. Furthermore, samples with fly ash replacement exhibit a lower slope of bulk resistivity as compared with samples without fly ash. Fig.6 shows the resistivity  $\rho$  change up to 24 hours on the logarithmic scale which identifies the turning point  $P_t$  and more critically the rate of change of resistivity,  $K_m$ . The time corresponding to point  $P_t$  for mixes FA0, FA10, and FA20 was 601, 632, and 665 min respectively. The points  $\rho_m$  and  $P_t$  divide the hydration process into three stages of dissolution, setting and hardening.

From mixing until the minimum resistivity, the

Table 2 Critical points from experimental measurements

Sample	Rheological measurement		Electrical measurement		Setting time	
	Slope, $K$ Pa/min	$\tau_0$ /Pa	$\rho_m$ /( $\Omega\cdot m$ )	$K_m$ /( $\Omega\cdot m/min$ )	Initial, $t_i/min$	Initial, $t_f/min$
FA0	0.01105	136	0.521	5.736	228	318
FA10	0.008648	219	0.581	4.997	275	367
FA20	0.006190	317	0.631	4.259	294	414

resistivity will reduce gradually due to the presence of Potassium, sodium, calcium, hydroxyl and sulphate ions that are released from the paste. The higher resistivity of sample FA20 shows that fewer ions are released into the solution. The minimum point  $\rho_m$  is at 71, 73, and 82 min for samples FA0, FA10, and FA20 respectively. The delay in the occurrence of  $\rho_m$  indicates that fly ash used has a dilution effect. From the minimum resistivity, the electrical resistivity increases slightly up to the transition point  $P_t$ . This period corresponds to the setting process and a gradual decrease in porosity and an increase in tortuosity.

The general equation from the fitting lines for each curve is shown in Eq.(5):

$$\rho(t)=K_m \cdot \ln(t)+d \tag{5}$$

The differential form of Eq.(5) is shown in Eq.(6):

$$\frac{\partial \rho}{\partial (\ln t)}=K_m \tag{6}$$

where,  $K_m$  represents the rate of densification of the cementitious matrix in unit volume. The influence of fly ash volume on the rate of densification  $K_m$  and  $d$  for different curves is calculated in Eqs.(7-9) and listed in Table 2.

$$\text{FA0:} \quad \rho=5.736 \ln t-36 \tag{7}$$

$$\text{FA10:} \quad \rho=4.997 \ln t-31.49 \tag{8}$$

$$\text{FA20:} \quad \rho=4.259 \ln t-27 \tag{9}$$

The logarithmic Eq.(5) predicts the trend of electrical resistivity during the deceleration period. The paste with a higher fly ash replacement has a lower  $K_m$  value. The lower  $K_m$  values in the FA samples reveal the replacement effect of fly ash after hardening.

### 3.3 Fluidity

The spread diameter of cement paste decreases

by 20 mm from 110 mm when the fly ash replacement varies from 0% to 20%. At an intermediate value of 10% replacement of cement with fly ash, the spread is 100 mm. Fig.7 shows the correlation between the initial yield stress  $\tau_0$  measured using a rheometer and the diameter of spread  $D$  from mini slump cone.

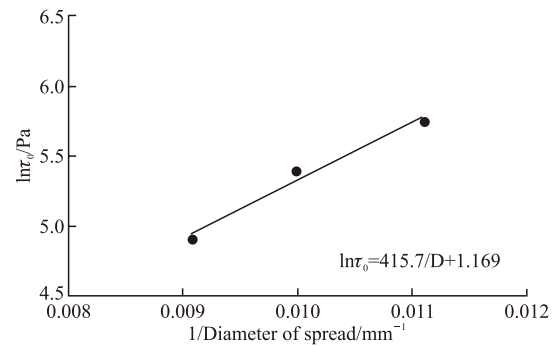


Fig.7 Correlation of initial yield stress  $\tau_0$  measured using a rheometer and diameter of spread  $D$  from mini slump cone

It is evident that the spread decreases with increasing fly ash addition-the influence of fly ash on spread shows mixed results depending on the composition of the fly ash, for instance literature<sup>[23]</sup> found an increase in the spread diameter when a class F fly ash was used although the mixture incorporated superplasticizer. Roussel *et al*<sup>[13]</sup> proposed a linear inverse relationship between the diameter of spread and the yield stress. Furthermore, a mathematical relationship between the initial yield stress and the diameter of spread from the mini cone is given in Eq.(10):

$$\ln \tau_0 = \frac{415.7}{D} + 1.168 \tag{10}$$

### 3.4 Setting time and compressive strength

Figs.8(a) and 8(b) represent the setting time and compressive strength of all the samples respectively. Fly ash delays the hydration process as evidenced in this study by the delay in setting time and compressive strength.

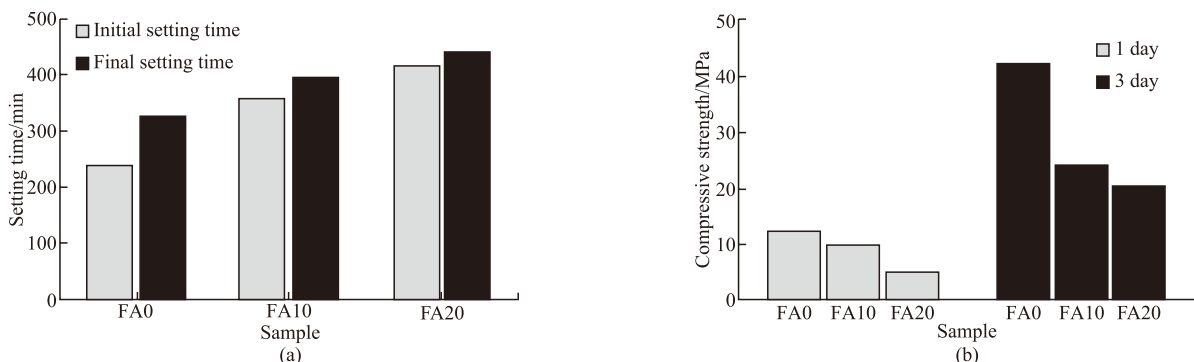


Fig.8 Influence of fly ash dosage on (a) setting time (b) compressive strength at 1 day and 3 days

These two parameters are commonly used to decide the choice of concrete mix to be used for a particular project. Sample FA0 with no fly ash replacement has the earliest initial and final setting time and the highest compressive strength at 1 day and 3 days. The influence of fly ash on these two parameters has been studied<sup>[24]</sup> and the retardation effect was found.

### 4 Analysis of results

Fig.9 shows the correlation between the slope of yield stress ( $K$ ) and the average slope of electrical resistivity ( $K_m$ ).

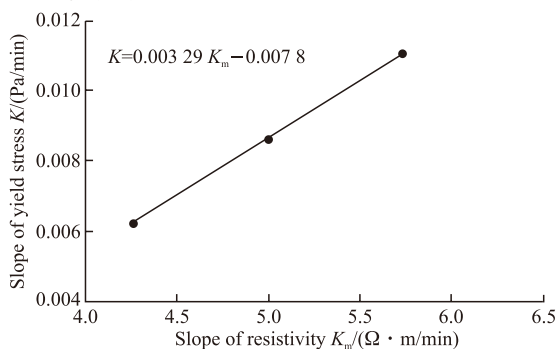


Fig.9 Correlation between the slope of yield stress ( $K$ ) and the average slope of electrical resistivity ( $K_m$ )

From Fig.9, the relationship in Eq.(11) is put forward. It can be seen that the slope of the yield stress  $K$  is linearly positive with the slope of resistivity,  $K_m$ :

$$K = 0.00329K_m - 0.0078 \tag{11}$$

Eqs.(10) and (11) are substituted into Eq.(1) to

obtain the general solution in Eq.(12):

$$\ln(t) = (0.00329K_m - 0.0078)t + \frac{415.7}{D} + 1.168 \tag{12}$$

where,  $K_m$  is the slope of the electrical resistivity curve ( $\Omega \cdot m/min$ ),  $t$  is time (min), and  $D$  is the diameter of spread from the mini cone (mm).

Eq.(12) can be used as an alternative method to estimate the yield stress of cement paste development with time.

The microstructure was observed at 3 days using a scanning electron microscope and the filler effect is evidenced by the un-reacted spherical fly ash particles in sample FA20 as shown in Fig.10(b). The fly ash used for filler had a lower  $K_m$  as shown in Fig.10(a).

After a certain period of time, the hydration products have accumulated enough for the particles to start clustering and as such the volume of solids (cement and hydration products) increases while the volume of water decreases and thus the yield stress drastically increases. However, the conductive path of electricity has not been blocked; this explains the delay in the increase of resistivity in comparison with the yield stress. The influence of fly ash on this process is reflected in Fig.6 where FA10 and FA20 have a lower  $K_m$  value than that of FA0 without fly ash.

### 5 Conclusions

In this study, the yield stress development of samples containing 0%, 10%, and 20% fly ash was tested and compared quantitatively with the resistivity

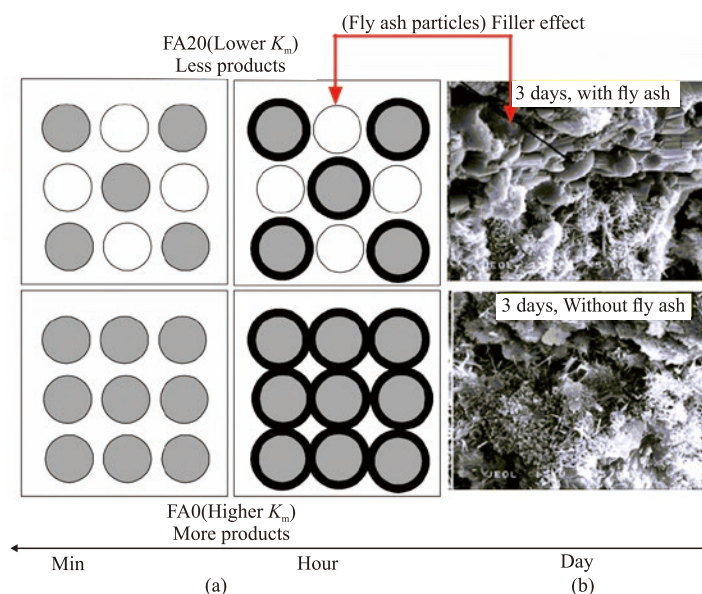


Fig.10 The filler effect of fly ash when used as a replacement in a cement system (a) minutes and hours after mixing more hydration products formed in FA0 (b) SEM image at 3 days showing less C-S-H (spiky) in ample FA20

development. Within the limits of this experiment, the following conclusions can be drawn:

a) Yield stress growth for samples with varying amounts of fly ash has the same shape, with a gradual increase in yield stress followed by a drastic increase after a critical time, which indicates the onset of acceleration and initial setting time as detected by a rheometer. This time is earlier than the initial setting time detected by a vicat needle and acceleration period detected by electrical resistivity measurements implying a higher sensitivity.

b) The percolation of solid phase in the hydrating cement can satisfactorily explain the drastic increase in yield stress and the delay in critical time  $\tau_c$  with increasing amounts of fly ash. The filler effect of fly ash is seen as dominating and is responsible for the retardation in hydration process as evidenced by the setting time and compressive strength at 1 day and 3 days.

c) This study proposes adopting the diameter of spread  $D$  and rate of resistivity  $K_m$  to predict the growth of yield stress. There is a positive relationship between the slope of yield stress  $K$  and the average slope of electrical resistivity  $K_m$ . The conductive channels of paste are gradually blocked, so electrical resistivity begins to increase after the dissolution stage. Both yield stress and electrical resistivity are controlled by porosity decrease and the clustering of the particles.

## References

- [1] Grzeszczyk S, Lipowski G. Effect of Content and Particle Size Distribution of High-Calcium Fly Ash on the Rheological Properties of Cement Pastes[J]. *Cement and Concrete Research*, 1997, 27(6): 907-916
- [2] Bouzouba N, Lachemi M. Self-Compacting Concrete Incorporating High Volumes of Class F Fly Ash: Preliminary Results[J]. *Cement and Concrete Research*, 2001, 31(3): 413-420
- [3] Uchikawa H, Uchida S, Ogawa K. Influence of Fly Ash Characteristics on the Rheological Properties of Fresh Fly Ash Cement Paste[C]. In: *Proceedings of the Symposium of the Materials Research Society*, Boston, Massachusetts, 1982
- [4] Li ZJ, Zhang D, Wu KR. Cement-based 0-3 Piezoelectric Composites[J]. *Journal of the American Ceramic Society*, 2002, 85(2): 305-313
- [5] AiadI, Abd El-Aleem S, El-Didamony H. Effect of Delaying Addition of Some Concrete Admixtures on the Rheological Properties of Cement Pastes[J]. *Cement and Concrete Research*, 2002, 32(11): 1 839-1 843
- [6] Banfill PFG. Rheology of Fresh Cement and Concrete[C]. In: *Proceedings of an International Conference, Liverpool*, 1990: CRC Press
- [7] Schultz MA, Struble LJ. Use of Oscillatory Shear to Study Flow Behavior of Fresh Cement Paste[J]. *Cement and Concrete Research*, 1993, 23(2): 273-282
- [8] Saasen A, Marken C, Dawson J, et al. Oscillating Rheometer Measurements on Oilfield Cement Slurries[J]. *Cement and Concrete Research*, 1991, 21(1): 109-119
- [9] Rafalski L. Rheological Properties of Fresh Bentonite-Cement Slurries Modified by Selected Sodium Salts[J]. *Archives of Civil Engineering*, 1995, 41(4): 551-553
- [10] Sant G, Ferraris CF, Weiss J. Rheological Properties of Cement Pastes: A Discussion of Structure Formation and Mechanical Property Development[J]. *Cement and Concrete Research*, 2008, 38(11): 1 286-1 296
- [11] Saak AW, Jennings HM, Shah SP. A Generalized Approach for the Determination of Yield Stress by Slump and Slump Flow[J]. *Cement and Concrete Research*, 2004, 34(3): 363-371
- [12] Amziane S, Ferraris CF. Cementitious Paste Setting Using Rheological and Pressure Measurements[J]. *ACI Materials Journal*, 2007, 104(2): 137-145
- [13] Roussel N, Stefani C, Leroy R. From Mini-Cone Test to Abrams Cone Test: Measurement of Cement-Based Materials Yield Stress Using Slump Tests[J]. *Cement and Concrete Research*, 2005, 35(5): 817-822
- [14] Bhattacharja S, Tang FJ. Rheology of Cement Paste in Concrete with Different Mix Designs and Interlaboratory Evaluation of the Mini-Slump Cone Test[J]. *PCA R&D, Serial*, 2001(2412): 121-124
- [15] Backe KR, Lile OB, Lyomov SK. Characterising Curing Cement Slurries by Electrical Conductivity[C]. In: *SPE Western Regional Meeting, Society of Petroleum Engineers*, 1998
- [16] Powers TC. Structure and Physical Properties of Hardened Portland Cement Paste[J]. *Journal of the American Ceramic Society*, 1958, 41(1): 1-6
- [17] Balshin MY. Relation of Mechanical Properties of Powder Metals and Their Porosity and The Ultimate Properties of Porous Metal-Ceramic Materials[J]. *Dokl. Akad. Nauk SSSR.*, 1949: 831-834
- [18] Xiao LZ, Li ZJ. Early-age Hydration of Fresh Concrete Monitored by Non-Contact Electrical Resistivity Measurement[J]. *Cement and Concrete Research*, 2008, 38(3): 312-319
- [19] Wei XS, Xiao LZ, Li ZJ. Study on Hydration of Portland Cement Using an Electrical Resistivity Method[J]. *Guisuanyan Xuebao(Journal of the Chinese Ceramic Society)(China)*, 2004, 32: 34-38
- [20] Nguyen QD, Boger DV. Measuring the Flow Properties of Yield Stress Fluids[J]. *Annual Review of Fluid Mechanics*, 1992, 24(1): 47-88
- [21] Brookfield. <http://www.brookfieldengineering.com/download/files/RSBro.pdf>.
- [22] Li ZJ, Li W. Contactless. *Transformer-based Measurement of the Resistivity of Materials*[P]. US,US6639401. 2003
- [23] Güneyisi E, Gesoglu M, Al-Goody A, et al. Fresh and Rheological Behavior of Nano-Silica and Fly Ash Blended Self-Compacting Concrete[J]. *Construction and Building Materials*, 2015, 95: 29-44
- [24] Wei XS, Li ZJ. Study on Hydration of Portland Cement with Fly Ash Using Electrical Measurement[J]. *Materials and Structures*, 2005, 38(277): 411-417